Laser-tuned whispering gallery modes in silica microbubble resonator integrated with iron oxide particles*

LIANG Cong-zhou (梁从周)[1], **ZHANG Hao** (张昊)[1]**, **WANG Yu-jia** (王羽佳)[1], **WU Ji-xuan** (吴继旋)[2], **LIN Wei** (林炜)[1], **LIU Bo** (刘波)[1], **and LIU Hai-feng** (刘海锋)[1]

1. Tianjin Key Laboratory of Optoelectronic Sensor and Sensing Network Technology, Institute of Modern Optics, Nankai University, Tianjin 300350, China

2. Tianjin Key Laboratory of Optoelectronic Detection Technology and Systems, College of Electronic and Information Engineering, Tianjin Polytechnic University, Tianjin 300387, China

(Received 19 January 2020; Revised 11 February 2020)

A 473-nm-laser-tuned whispering gallery mode (WGM) silica microbubble resonator integrated with iron oxide particles is demonstrated in this paper. Owing to the photo-induced thermal effect, the WGM resonance wavelength could be tuned by adjusting laser power density of the illuminating light absorbed by the iron oxide particles. A wavelength tuning sensitivity of 0.03 nm/(mW·mm^{-2}) and a tuning range of 0.18 nm are experimentally achieved. Moreover, the influence of ambient temperature on the WGM spectral characteristics is experimentally studied, and a silica-microbubble-based reference scheme is demonstrated to compensate for the temperature-caused resonance wavelength variation. The proposed laser-tuned microresonator has great potential in optical modulation and high-precision optical filtering applications.

Document code: A **Article ID:** 1673-1905(2021)03-0129-5

DOI https://doi.org/10.1007/s11801-021-0012-y

Due to their desirable advantages such as highquality factor, small mode volume and compact size, whispering gallery mode (WGM) microresonators have been investigated in numerous studies and applications, such as optical tuning[1-3], bio-sensing[4-6], and microcavity laser[7,8]. WGM resonance wavelength could be tuned by controlling optical properties of the microcavity, and several tuning methods have been studied in the recent years[9-11]. Particularly, all-optical tuning of WGMs is highly attractive in optical switching and optical filtering applications despite the weak Kerr effect and absence of plasma dispersion effect in silica-based microresonators. To overcome these disadvantages, functional materials such as magnetic fluids (MFs) could be integrated with the microresonators to improve the WGM tunability. In 2014, an all-optical control scheme based on optofluidic ring resonator is firstly demonstrated by Liu et al[12]. By infiltrating MFs into the microcapillary, the illuminating light could be strongly absorbed, leading to wavelength shift of WGM resonance dips. And a few years later, Deng et al achieved broadband laser tuning based on a micro-structured optical fiber microresonator embedded with iron oxide nanoparticles[13]. As solid state iron oxide nanoparticles serve as functional materials, the influence of the liquid flow on device performances could be avoided. Apart from the tuning methods based on photothermal effect, in 2017, Li et al developed a laser-tuned microsphere resonator integrated with ethyl-orange-doped coating[10] by exploiting the reversible photo-isomerization effect of ethyl orange molecules. However, in their schemes, the Q-factors of the microresonators are less than 10^5, which may be relatively insufficient for specific applications.

In this paper, we propose and experimentally demonstrate a laser-tuned silica microbubble WGM resonator integrated with iron oxide particles. The iron oxide particles serve as the thermal absorption medium, and their photo-induced thermal effect would cause thermal expansion and refractive index (RI) variations of silica materials to change optical properties of the microresonator. WGM resonance wavelength dependence on 473 nm laser power density has been experimentally investigated, and a wavelength tuning sensitivity of 0.03 nm/(mW·mm^{-2}) is achieved. Besides, experimental results indicate that the influence of ambient temperature on the WGM resonance wavelength is not negligible, which may undermine the tuning performances of the proposed microresonator. To overcome this issue, a hollow microbubble is employed as a dynamic reference to compensate for the variation of ambient temperature. Our proposed microbubble resonator integrated with iron oxide particles (MIIOP) possesses

* This work has been supported by the National Natural Science Foundation of China (Nos.11774181, 61875091, 11904262, 11904180, 61727815 and 11274182), and the Natural Science Foundation of Tianjin (No.19JCYBJC16700).

** E-mail: haozhang@nankai.edu.cn

such desirable features as high Q-factor and ease of fabrication, which makes it a good candidate for applications in tunable optical filtering and optical modulation.

Fig.1(a) shows the micrograph of the microbubble employed in our experiment. The microbubble is fabricated from a silica microcapillary, whose inner and outer diameters are 50 μm and 125 μm, respectively. To produce a microbubble, one end of the microcapillary is sealed while an air pump is employed at the other end to apply certain pressure on the inner wall. Then electric arcs are applied at the middle point of the microcapillary by using a fusion splicer (S178A, produced by Furukawa Electric Co., Ltd., Japan). By changing arc charge and air pressure, microbubbles of different sizes could be fabricated. Iron oxide particles are embedded on the inner wall of the microbubble by drying the magnetic fluids filled in the microbubble. After the evaporation of the base solution, a film of iron oxide particles is formed, as shown in Fig.1(b).

Fig.2 shows a schematic diagram of the WGM excitation and test system. The transmission spectral loss measurement system consists of a tunable laser (TL, 8164B produced by Keysight Technologies, US) with an operation wavelength range of 1 530 nm to 1 560 nm, a polarization controller (PC, N7786B produced by Keysight Technologies, US) and an optical power meter (OPM, N7744A produced by Keysight Technologies, US). In the meanwhile, the above devices are all connected to a laptop for parameter control and data processing. The MIIOP is placed in contact with a tapered fiber with a diameter of 1.5 μm. Due to the mode overlapping between the evanescent field of the tapered fiber and the WGMs of the microresonator, part of the light would be coupled into the WGMs in the microresonator. Consequently, resonance dips would emerge in the transmission spectrum of the tapered fiber. A 473 nm laser (MBL-N-473-1W, produced by Changchun New Industries Optoelectronics Tech Co., Ltd., China) and a variable optical attenuator (VOA) are employed to provide lateral laser illumination.

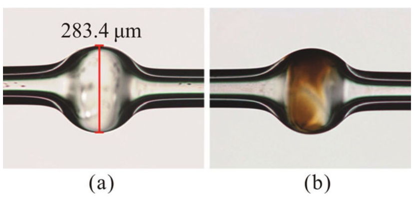

Fig.1 Micrographs of the silica microbubble (a) before and (b) after being integrated with iron oxide particles

Fig.3 shows the transmission spectrum of the WGM system without applying the illuminating light. The resonance dip 1 548.65 nm is selected for monitoring of wavelength shift. It could be seen that the free spectrum range (*FSR*) is ~1.93 nm. As shown in Fig.4, Lorentz fitting is performed on the resonance dip spectrum, and the Q-factor is calculated to be 3.02×10^5 according to

$$Q=\frac{\Delta\lambda}{\lambda}, \tag{1}$$

where λ is resonance wavelength and $\Delta\lambda$ is the full width at half maximum (*FWHM*).

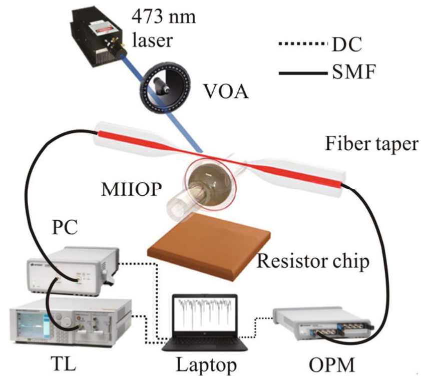

Fig.2 Schematic diagram of the WGM excitation and test system (The dashed and solid lines refer to data cables and single-mode fibers, respectively.)

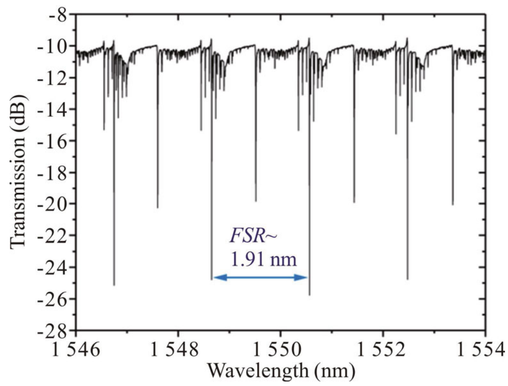

Fig.3 Transmission spectrum of the MIIOP

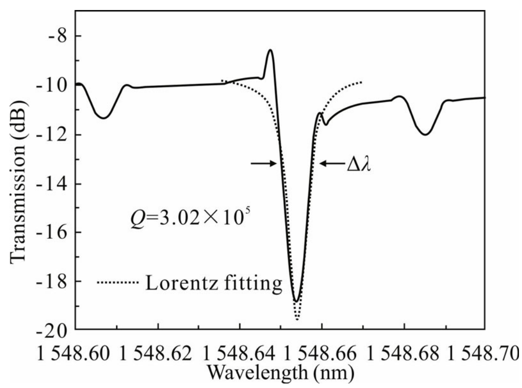

Fig.4 Enlarged transmission spectrum around the resonance dip

As linearly polarized light from the PC enters the tapered region of the microfiber, WGMs could be excited owing to the coupling between evanescent field of the tapered fiber and WGMs of the microbubble. WGM resonance wavelengths should satisfy the following resonance condition:

$$m\lambda=2\pi n_{\rm eff}R, \tag{2}$$

where λ is resonance wavelength, n_{eff} refers to effective refractive index, m is an integer, and R represents radius of the microbubble. Under laser illumination, the iron oxide particles would absorb the incident light to heat up the microresonator. Consequently, n_{eff} and r_{eff} would vary due to thermal-optic and thermal expansion effects, as described by the following equations:

$$n_{eff} = n_{eff}^0(1+\xi\Delta T) = n_{eff}^0(1+\xi\eta p) \ , \quad (3)$$

$$r_{eff} = r_{eff}^0(1+\alpha\Delta T) = r_{eff}^0(1+\alpha\eta p) \ , \quad (4)$$

where ξ and α represent the thermal-optic and thermal expansion coefficients of pure silica with their respective values of 8.3×10^{-6} and 5.5×10^{-7}, η refers to the correlation coefficient between temperature and laser power density, n_{eff}^0 and r_{eff}^0 are defined as initial effective refractive index and effective radius without light illumination, respectively. And therefore, the resonance wavelength sensitivity could be expressed as:

$$S = \frac{\partial\lambda}{\partial p} = \frac{(\alpha+\xi)\lambda\eta}{1-\frac{\lambda}{r_{eff}}\frac{\partial r_{eff}}{\partial\lambda}-\frac{\lambda}{n_{eff}}\frac{\partial n_{eff}}{\partial\lambda}} . \quad (5)$$

Since ξ and α are both positive, as laser with certain power density is applied onto the MIIOP, the WGM resonance dip would exhibit some red shift with the increment of laser power.

Fig.5 shows spectral evolution of the resonance dip under different laser power densities. It can be seen that with the increment of laser power density, resonance wavelength experiences some red shift, which is in accordance with our theoretical analysis based on Eq.(5). The depth of each resonance dip is about 7 dB, and the transmission loss fluctuations are smaller than 1.5 dB. Resonance wavelength shift as a function of applied laser power density for a range of 0 to 5.9 mW/mm^2 is shown in Fig.6, and error bars acquired through repeated measurements are also given in this figure, which are acceptable for practical applications. Linear fitting results according to the experimental data show that the proposed MIIOP possesses a resonance wavelength tuning sensitivity of 0.03 nm/(mW·mm^{-2}) with good linear responsivity.

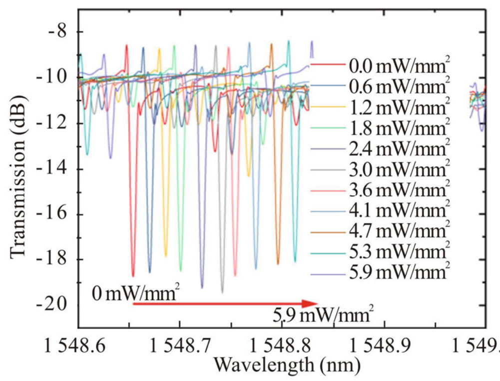

Fig.5 WGM spectral evolution for different applied laser power densities

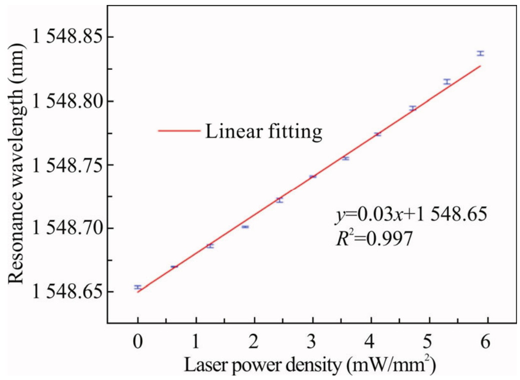

Fig.6 WGM resonance wavelength shift as a function of applied laser power density

We have also experimentally investigated the influence of ambient temperature on resonance wavelength. To control the ambient temperature, a resistor chip is placed close to the microbubble resonator and a DC power supply is applied on the chip. An infrared thermometer is employed to monitor the chip temperature in real time and ensure that the environmental temperature is stable during the experimental process. Experimental results indicate that the resonance dip moves toward longer wavelength region as ambient temperature increases, and the linear fitting result indicates linear correlation between them, as shown in Fig.7. It should be noted that both of light absorption and ambient temperature variation would affect wavelength tuning performances. Further experimental results show that wavelength shift can be regarded as the sum of light-caused shift and ambient-temperature-caused shift. Fig.8 gives WGM resonance shift as a function of applied laser power density under different ambient temperatures. It can be seen that light tuning sensitivity maintains almost unchanged at 25 °C and 50 °C.

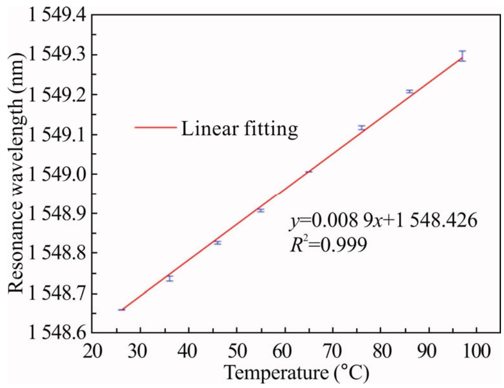

Fig.7 WGM resonance wavelength as a function of ambient temperature

However, as the experimental results indicate, the influence of ambient temperature on resonance wavelength is not negligible, which may degrade the wavelength tuning performances of the proposed MIIOP. To resolve this problem, wavelength tuning performances of a microbubble without iron oxide particles have been experimentally investigated. Resonance wavelength shift as functions of laser power density and ambient temperature for this kind of microbubble are shown in Fig.9 and Fig.10, respectively. From Fig.9, it can be seen that without the photothermal effect of iron oxide particles, resonance dip of the microbubble resonator exhibits some wavelength fluctuation less than 5 pm for different applied laser power densities. Thus it can be concluded that illuminating light does not have obvious impact on the resonance wavelength. However, as presented in Fig.10, linear fitting result indicates the wavelength tuning sensitivity is 0.006 8 nm/°C, which is slightly lower than that of the MIIOP employed in this study. Therefore, the microbubble resonator without iron oxide particles could be utilized as a dynamic reference only sensitive to ambient temperature.

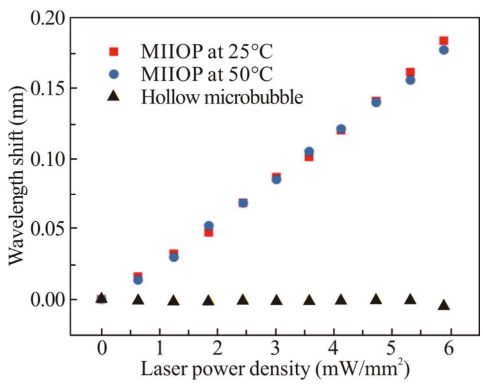

Fig.8 WGM resonance wavelength shift as a function of laser power density at different temperatures

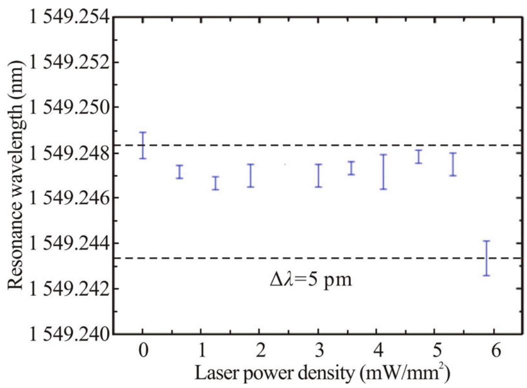

Fig.9 WGM resonance wavelength shift as a function of applied laser power density for the microbubble resonator without iron oxide particles

To compensate for the temperature effect, the microbubble without iron oxide particles should be placed close to the MIIOP so that ambient temperature is the same for the two microbubbles. Resonance wavelength shift of the above microbubble resonators as functions of laser power density and ambient temperature can be described by the following matrix equation:

$$\begin{bmatrix} S_1 & S_2 \\ 0 & S_3 \end{bmatrix}\begin{bmatrix} P \\ \Delta T \end{bmatrix}=\begin{bmatrix} \Delta\lambda_1 \\ \Delta\lambda_2 \end{bmatrix}, \qquad (6)$$

where $\Delta\lambda_1$ and $\Delta\lambda_2$ are resonance wavelength shifts of MIIOP and the microbubble without iron oxide particles, respectively, S_2 and S_3 refer to their respective wavelength tuning sensitivities to ambient temperature, S_1 represents wavelength tuning sensitivity to laser power density of the MIIOP, P is laser power density and ΔT is ambient temperature change. From Eq.(6), it can be deduced that $\Delta\lambda_1$ can be expressed as:

$$\Delta\lambda_1 = S_1 P + \frac{S_2}{S_3}\Delta\lambda_2 = 0.03P + 1.31\Delta\lambda_2 \ . \qquad (7)$$

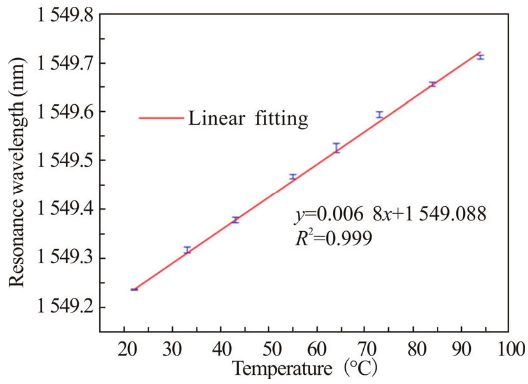

Fig.10 WGM resonance wavelength shift as a function of ambient temperature for the microbubble resonator without iron oxide particles

As ambient temperature variation occurs, it is possible to adjust the light power accordingly to make the resonance wavelength of MIIOP remain unchanged. This could be exploited as an effective method to compensate for the temperature effect in practical applications.

In this paper, a laser-tuned WGM tuning approach is proposed by employing a microbubble resonator integrated with iron oxide particles. The Q-factor of the microresonator reaches 3.02×10^5. Owing to strong absorption and photothermal effect of iron oxide particles, wavelength tunability of the microresonator under light illumination has been significantly enhanced, and a wavelength tuning sensitivity of 0.03 nm/(mW·mm^{-2}) has been experimentally acquired. Further experimental results indicate ambient temperature effect on WGM resonance wavelength, which is undesirable for practical wavelength tuning applications. In this case, another microbubble without iron oxide particles is employed as a reference to compensate for the temperature effect. Our proposed MIIOP possesses good tuning linearity, high Q-factor, showing a promising potential inhigh-precision optical filtering and all-optical wavelength tuning applications.

References

[1] Ilchenko V. S., Savchenkov A. A., Matsko A. B. and

Maleki L., Journal of the Optical Society of America B **20**, 333 (2003).
[2] Pacifici D., Lezec H. J. and Atwater H. A., Nature Photonics **1**, 402 (2007).
[3] Lin Wei, Zhang Hao, Liu Bo, Song Bin-bin and Liu Yan-ge, Scientific Reports **5**, 17791 (2015).
[4] Vollmer F. and Arnold S., Nature Methods **5**, 591 (2008).
[5] Arnold S., Shopova S. I. and Holler S., Optics Express **18**, 281 (2010).
[6] Ding Chang-qin, Zhu An-wei and Tian Yang, Accounts of Chemical Research **47**, 20 (2014).
[7] Francois A., Rowland K. J. and Monro T. M., Applied Physics Letters **99**, 141111 (2011).
[8] Goldenberg L. M., Lisinetskii V. and Gritsai Y., Advanced Materials **24**, 3339 (2012).
[9] Yang Cheng-kun, Zhang Hao, Liu Bo, Lin Shi-wei, Li Yue-tao and Liu Hai-feng, Optics Letters **42**, 2988 (2017).
[10] Li Yue-tao, Zhang Hao, Liu Bo, Lin Wei, Yan Dong-lin, Yang Cheng-kun and Wu Ji-xuan, Sensors & Actuators B Chemical **238**, 98 (2017).
[11] Aseel M., Vishnu K., Ahmed S. S., Peter K., Vlasta Z. and Gerald F., Optics Express **25**, 12195 (2017).
[12] Liu Yang, Shi Lei, Xu Xin-biao, Zhao Ping, Wang Zhe-qi and Pu Sheng-li, Lab on a Chip **14**, 3004 (2014).
[13] Deng Ming, Wang Yu-fan, Liu Lei-guang and Qin Mao-ru, Applied Optics **57**, 4563 (2018).